



## King's Research Portal

DOI:

[10.1016/j.ijpharm.2016.02.007](https://doi.org/10.1016/j.ijpharm.2016.02.007)

*Document Version*

Peer reviewed version

[Link to publication record in King's Research Portal](#)

*Citation for published version (APA):*

Cai, X. J., Patel, T., Woods, A., Mesquida, P., & Jones, S. A. (2016). Investigating the influence of drug aggregation on the percutaneous penetration rate of tetracaine when applying low doses of the agent topically to the skin. *INTERNATIONAL JOURNAL OF PHARMACEUTICS*, 502(1-2), 10-17. <https://doi.org/10.1016/j.ijpharm.2016.02.007>

### **Citing this paper**

Please note that where the full-text provided on King's Research Portal is the Author Accepted Manuscript or Post-Print version this may differ from the final Published version. If citing, it is advised that you check and use the publisher's definitive version for pagination, volume/issue, and date of publication details. And where the final published version is provided on the Research Portal, if citing you are again advised to check the publisher's website for any subsequent corrections.

### **General rights**

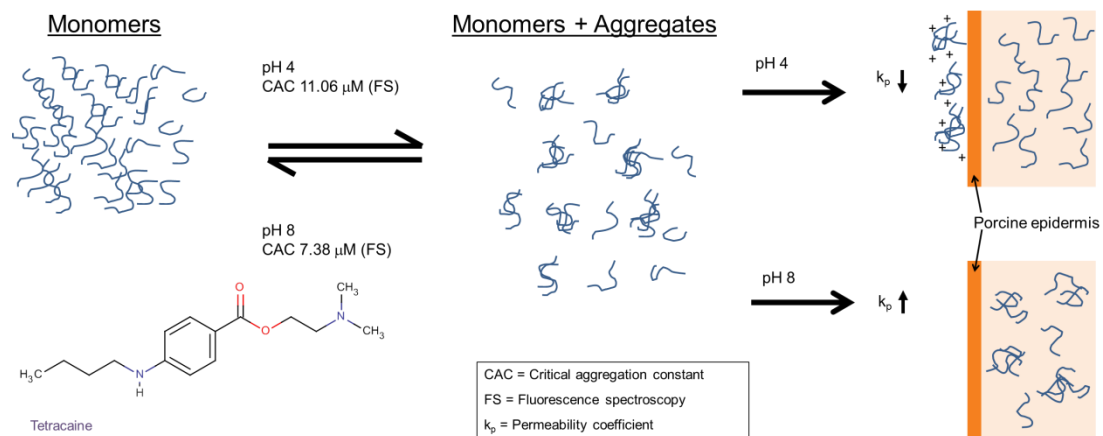
Copyright and moral rights for the publications made accessible in the Research Portal are retained by the authors and/or other copyright owners and it is a condition of accessing publications that users recognize and abide by the legal requirements associated with these rights.

- Users may download and print one copy of any publication from the Research Portal for the purpose of private study or research.
- You may not further distribute the material or use it for any profit-making activity or commercial gain
- You may freely distribute the URL identifying the publication in the Research Portal

### **Take down policy**

If you believe that this document breaches copyright please contact [librarypure@kcl.ac.uk](mailto:librarypure@kcl.ac.uk) providing details, and we will remove access to the work immediately and investigate your claim.

## Table of contents/ Abstract graphic



Investigating the influence of drug aggregation on the percutaneous penetration rate of tetracaine when applying low doses of the agent topically to the skin.

X. J. Cai, T. Patel, A. Woods, P. Mesquida, S. A. Jones\*

King's College London, Institute of Pharmaceutical Science, Franklin-Wilkins Building, 150 Stamford Street, London, SE1 9NH

International Journal of Pharmaceutics

(Impact factor 3.650, 2015 Journal Citation Reports)

**\*Corresponding author:** Dr. S. A. Jones. King's College London, Institute of Pharmaceutical Science, Franklin-Wilkins Building, 150 Stamford Street, London, SE1 9NH. Tel: +44 (0)207 848 4843. Fax: +44 (0)207 848 4800. E-mail: [stuart.jones@kcl.ac.uk](mailto:stuart.jones@kcl.ac.uk)

## **Abstract**

Understanding the molecular aggregation of therapeutic agents is particularly important when applying low doses of a drug to the surface of the skin. The aim of this study was to understand how the concentration of a drug influenced its molecular aggregation and its subsequent percutaneous penetration after topical application. A model drug tetracaine was shown to form a series of different aggregates across the  $\mu\text{M}$  (fluorescence spectroscopy) to  $\text{mM}$  (light scattering analysis) concentration range. The aggregate formation process was sensitive to the pH of the vehicle in which the drug was dissolved (pH 4, CMC – 11  $\mu\text{M}$ ; pH 8 CMC – 7  $\mu\text{M}$ ) and it appeared to have an impact upon the drug's percutaneous penetration. At pH 4, increasing the concentration of the drug in the donor solution decreased the skin permeability coefficient ( $K_p$ ) of tetracaine ( $13.7 \pm 4.3 \times 10^{-3} \text{ cm/h}$  -  $0.06 \pm 0.02 \times 10^{-3} \text{ cm/h}$ ), whilst at pH 8, it increased the  $K_p$  ( $29.9 \pm 9.9 \times 10^{-3} \text{ cm/h}$  –  $75.1 \pm 41.7 \times 10^{-3} \text{ cm/h}$ ). These data trends were reproduced in a silicone membrane and this supported the notion that the more polar aggregates formed at pH 4 acted to decrease the proportion of species available to pass through the skin, whilst the more hydrophobic aggregates formed in pH 8 increased the membrane diffusing species.

**Key words:** Tetracaine; transport; aggregation; skin; penetration enhancer; pain; drug delivery

## Introduction

Drug-vehicle interactions are known to have a significant influence on the ability of topically applied medicines to deliver actives into the skin [1, 2]. It has been previously shown that a certain degree of physical interaction between the active and the vehicle must occur to facilitate solubilisation of the drug, but if the physical interactions are too strong, then drug release from the product after application can be hindered [3].

Drug-drug interactions are in equilibrium with drug-vehicle interactions in topical products and therefore, drug-drug interactions may also have the potential to modify the performance of a medicine applied topically to the skin. Several therapeutic agents that are formulated in skin products are known to exhibit strong drug-drug interactions, which can lead to aggregation in the solution state, but how this molecular aggregation influences the potential of a drug to penetrate into the skin has not previously received a lot of attention [4-6].

Molecular aggregation is known to modify the physiochemical properties of a drug. For example, a drug's lipophilicity, molecular size, degree of ionisation, hydrogen bonding can all change upon the formation of drug aggregates. These physiochemical property modifications brought about by **concentration dependant** molecular aggregation can influence drug permeation directly by modifying the drug-skin interactions [7-10]. However, the skin is a highly restrictive barrier. Therefore, if drugs generate aggregate clusters with a size of larger than 10 nm, they would be unlikely to pass directly into the

skin unless they could access the follicular transport route [11-15]. Thus, in order to understand the influence of drug aggregation on percutaneous penetration, attempts must be made to characterise the drug aggregates formed when applied to the surface of the skin. In addition, to elucidate how these drug aggregates influence percutaneous penetration, due consideration must be given as to how they affect the availability of the membrane diffusing molecules.

Previous work has shown that when nano-sized drug aggregates are present in a solution added to the surface of the skin, they can slow down drug permeation [16]. This was assumed to be a consequence of the aggregation process reducing the quantity of free drug that was able to passively penetrate the membrane. In an ideal system, drug monomers would always be in equilibrium with the aggregated species and therefore, the interactions between the two systems may influence the quantity of molecules able to pass into the skin [17-19]. However, drug aggregation rarely follows the homogeneous process shown by simple surfactants due to the fact that their chemical structure is not designed specifically to confer amphiphilic properties like synthetic surfactant molecules. As a consequence, there is often not a single species of aggregate formed in solution. Rather, drugs can form different types of aggregates in a concentration dependant manner in a similar manner to polymers. This makes the interactions of these system hard to predict and it makes it feasible that the aggregation process could lead to either drug donor depletion during the transport of the drug [18, 20] or the availability of more molecules to take part in the transport process. [21, 22].

The aim of this project was to characterise the molecular aggregation of the model drug, tetracaine at low drug concentrations and to understand the influence of the molecular aggregation process on transmembrane transport. Tetracaine was selected as a model drug in this study because it is known to aggregate in aqueous solutions [4, 5]. In addition, it was selected as its clinical use is hindered by its high penetration lag time (30 to 45 minutes). Reducing lag time could improve the drugs performance in patients as it is often used before venepuncture or venous cannulation [23]. The focus of the study was to understand the aggregation process at low drug concentrations as it was suspected that the aggregates formed would be very different to the high concentrations previously assessed [16]. As a consequence, at low drug concentrations, tetracaine aggregation was characterised by three techniques: photon correlation spectroscopy, to correlate with the previous work, fluorescence spectroscopy, to assess aggregation at low drug concentrations and Fourier transform infrared spectroscopy (FTIR), to understand the intermolecular interactions. It was hoped that these three techniques would allow the drug aggregation process to be understood at drug concentrations ranging from the  $\mu\text{M}$  to the mM concentration range. The study compared tetracaine aggregation and percutaneous penetration in an aqueous vehicle set at pH 4 and pH 8 in order to assess if the ionisation of the drug would influence the aggregation and thus the percutaneous penetration. These two pHs were selected because tetracaine is a weak base with pKa's at the secondary and tertiary amine of 3.41 and 8.24 respectively at 32 °C. Using these pKa values at pH 4 it was predicted that 100 % of the tertiary amine would be ionised and 23 % of the secondary amine would be ionized, at pH 8 it was predicted that 72 % of the tertiary amine would be ionised and 28 % of tetracaine would be unionised. The drug transport

was studied using a porcine epidermis and a silicone membrane to understand the manner in which aggregation influences transport through barriers with and without the potential for follicular transport.

## **Materials and Methods**

### Materials

Tetracaine free base ( $\geq 98\%$ ) and hydrochloric acid were purchased from Sigma Aldrich, UK. Ultrapure water (18.2 M $\Omega$ ) was used throughout this study.

### Test sample preparation

Tetracaine solutions were prepared and adjusted to pH 4.0 or 8.0 using hydrochloric acid and equilibrated at 32 °C unless stated otherwise. Solutions were stirred for at least 24 h and the pH rechecked prior to analysis to ensure they were at equilibrium.

### Photon correlation spectroscopy

The derived count rates were analysed by photon correlation spectroscopy (Malvern Nanoseries Zetasizer ZEN3600, Malvern Instruments Ltd, UK). Detection of the light scattering signal was achieved at a 173 ° backscattering angle with samples equilibrated at 32 °C using water as a dispersant (refractive index 1.33, viscosity 0.8872 cP). Each



measurement comprised of 10-14 runs. Triplicates of each sample were assessed.

#### Fluorescence spectroscopy

Fluorescence emission spectra were recorded using a fluorescence spectrometer fitted with a Xenon pulse lamp (Varian Cary Eclipse Fluorescence Spectrometer, Agilent Technologies, UK). Beer-Lambert's law can only be applied over a limited range of optical densities and at a high sample optical density, attenuation due to absorption of the incident light or the emitted light can lead to a decrease in intensity and a possible change in spectral distribution [24, 25]. In light of the possibility of having a deviation in linearity due to the concentration of tetracaine and not the molecular aggregation, a Quartz fluorescence cells (Helima Fluorescence Cell, Helima UK Ltd., UK) with a 3 mm path length, with an off-centre illumination was used to record the measurements. Excitation and emission slits were fixed at 5 nm. In all measurements, the excitation wavelength was set at 310 nm. The samples were scanned from 320 to 450 nm at a wavelength scan rate of 120 nm/min with a PMT detector gain of 600 V. The data were smoothed with a Savitzky Golay function filter size 25 using the Cary Eclipse software. The experiments were performed at a temperature of 32 °C. The system was chemically stable over 6 days and the effect of ion pairing with the ions dissolved in the aqueous solution was not significant (Data not shown).

#### Critical aggregation concentration (CAC) analysis

Two methods were used to identify the CACs and their values were compared [26]. In

one of the methods, a second derivative function was applied to the data by using OriginPro (OriginPro version 8.6, Origin Lab Corporation, US). The data was fitted with a non-linear model before a Gaussian distribution function was applied to highlight the critical points, i.e. the regions where local minimum or maximum occurred. In the other method, the intersection of 2 linear models that were applied to the data was determined. The second of these two methods is traditionally used when determining the CMC of surfactants [27].

#### FTIR analysis

Deuterated water (D<sub>2</sub>O, Sigma Aldrich, UK) was employed to analyse the tetracaine solutions as it dampened the solvent signal in the 1700 – 1300 cm<sup>-1</sup> and 3000 – 2850 cm<sup>-1</sup> ranges. The samples were loaded into a demountable universal transmission cell system (Omni-Cell, Specac Ltd, UK) fitted with CaF<sub>2</sub> windows and a 25 µm Mylar spacer (Specac Ltd., UK). The pHs of the tetracaine solutions were maintained using DCl. All spectra were produced using 32 scans collected at a spectral resolution of 4 cm<sup>-1</sup>. The data was recorded using a Spectrum One spectrometer (Perkin-Elmer Ltd., UK) and analyzed with Spectrum software (version 10, Perkin-Elmer Ltd., UK).

#### Tetracaine transport studies

Two barriers were employed for the transport studies, silicone membrane (0.12 mm, GBUK Healthcare, UK, no pre-treatment required) and porcine epidermis. Fresh

untreated white adult porcine ears were obtained from a local abattoir (Evans and Sons, UK). Damaged ears were discarded. After cleaning under clear running deionized water and wiping the residue with clean wipes, visible hairs were trimmed carefully. The preparation of epidermal porcine skin was carried out by heat separation [28]. Porcine skin were immersed and gently stirred in deionised water at 60 °C for 1 min. After removal from the deionized water, the skin was put on a corkboard with the dermal side down and the epidermis was carefully separated from the dermis with tweezers. The separated epidermis was washed with deionized water and floated on filter paper (Whatman no. 1, UK) to act as a support. The samples were wrapped in aluminium foil and stored at - 20 °C for a maximum of up to 1 month [29]. The samples were thawed before use.

The transport studies were carried out using upright individually calibrated Franz diffusion cells with an average surface area of  $2.1 \pm 0.1 \text{ cm}^2$  and receptor compartment volume of  $9.2 \pm 0.5 \text{ mL}$ . The barrier was cut, mounted and sealed with parafilm between two chambers of the glass diffusion cell with a 13 mm magnetic flea in the receiver chamber. The cells were inverted and filled with previously filtered and sonicated receiver fluid. A solution pH adjusted to pH 4.0 and 8.0, with HCl, was used as a receiver fluid for the silicone membrane transport studies to investigate the transport of tetracaine through a hydrophobic barrier. Phosphate buffered saline (pH 7.4) was employed as a receiver fluid for the porcine epidermis transport studies to mimic the skin environment. The transport studies were performed on a submergible magnetic stirrer plate in a pre-heated water bath set at 37 °C to provide a membrane surface temperature of 32 °C. After

cell equilibration for 1 h, the cells were checked for leaks by inversion and visual inspection for back diffusion. Infinite doses (i.e. > than the classical 2-5 mg / cm<sup>2</sup> used to mimic dosing in vivo) of tetracaine mixtures (1 mL) were applied uniformly to the surface of each membrane so that a good representation of flux could be gained without significant donor phase depletion. The donor compartment was covered with a parafilm to minimise donor phase evaporation. At predetermined time intervals, 1 mL aliquots were removed from the receiver phase and replaced with fresh receiver fluid to keep the liquid volume in the receiver compartment constant. The collected samples were analysed by HPLC. A total of 5 replicates of each experiment were performed.

Cumulative amounts of drug (ng) penetrating the unit surface of the membrane area (cm<sup>2</sup>) were corrected for sample removal and plotted against time (h). The steady-state flux (J) was calculated from the slope of the linear portion of the curve ( $R^2 \geq 0.98$ ), using at least 4 points with values above the assay [limit of quantification \(LOQ\)](#). The permeability coefficient of tetracaine was calculated using equation 1 [30]:

$$J = \frac{k_p}{C_v} \quad (\text{Equation 1})$$

where J represents the flux,  $K_p$  is the permeability coefficient of the permeant across the membrane and  $C_v$  is the concentration of the drug in the vehicle. The enhancement ratio (ER) due to the various additives were determined using the following equation:

$$ER = \frac{J_2}{J_1} \quad (\text{Equation 2})$$

where  $J_1$  and  $J_2$  are the steady-state transmembrane transport rate of tetracaine from the tetracaine and tetracaine-nanoparticle mixture respectively. Drug concentration and not drug thermodynamic activity was used throughout this study to set the drug levels in the experiments and discuss the data because it was not the intention of this study to directly compare the drug flux at pH 4 and pH 8, this has been published in previous work (16), rather the study sought to compare the trends within each different vehicle. The data display and interpretation reflected this important feature of the study design.

#### Tetracaine quantification

The quantification of tetracaine was performed using a reverse-phase HPLC system consisting of a pump with autosampler (Hewlett-Packard series 1050, Agilent Technologies UK Ltd., UK) connected to a fluorescence detector (Shimadzu detector RF-551, Shimadzu corp., Japan). The system was controlled via a computer with Chromeleon software (Dionex Corp., USA), which was also used to record and interpret the analytical data. The mobile phase comprised acetonitrile-methanol-acetate buffer (0.1 M) (25:25:50 (v/v), pH 5.1) set at a flow rate of  $1.0 \text{ mL}\cdot\text{min}^{-1}$ . Tetracaine was separated using a Luna 3  $\mu\text{m}$  C18(2) (150 X 4.6 mm) stationary phase (Phenomenex, UK) at room temperature with a 100  $\mu\text{L}$  injection volume and the fluorescence detection at an excitation wavelength of 310 nm and an emission wavelength of 372 nm. The retention time for tetracaine was 4.2 min. The calibration curves were constructed on the basis of the peak area measurements using standard solutions of known tetracaine concentrations dissolved

in an identical fluid as the receiver phase for the transport studies,  $10^{-4}$  HCl (pH 4 water). The assay was shown to be “fit for purpose” in terms of sensitivity (LOD – 4.08 ng/mL, LOQ – 74 ng/mL, n=25), precision (6 % CV), and linearity ( $R^2 \geq 0.99$ ).

### Statistical Analysis

All values were expressed as their mean  $\pm$  standard deviation (SD). The statistical analysis of data was performed using the statistical package for social sciences, SPSS version 21, (IBM Corp., USA) with a significance level of 0.05. The normality (Sapiro-Wilk) and homogeneity of variances (Levene’s test) of the data were assessed prior to statistical analysis. Transport data were analysed statistically using one-way analysis of variance (ANOVA) tests for normally distributed data and a non-parametric Kruskal-Wallis tests for non-Gaussian distributed data. Post hoc comparisons of the means of individual groups were performed when appropriate using Dunnet’s test for normal distributed data and Games Howell test for non-Gaussian distributed data. For all pair-wise comparison of means, Student’s independent t-test or Mann-Whitney test was applied. Data were presented using OriginPro software (OriginPro version 8.6, OriginLab Corporation, US).

## Results

### Tetracaine aggregation

Tetracaine aggregation in the mM region was determined by photon correlation spectroscopy (Table 1). By applying a second derivative function to the plot of the tetracaine solution concentration vs the unattenuated light scattering signal (derived count rates), the first critical point (defined as the CAC in this methodology) significantly decreased ( $p < 0.05$ ) from 40 to 0.3 mM when the pH increased from 4 to 8. A similar trend of decreasing CAC as a function of increasing pH was observed when the intersection method was used to determine the CAC (Fig. 1), i.e., the CACs significantly decreased ( $p < 0.05$ ) from 95.10 mM in pH 4 to 2.91 mM in pH 8. As there was not a sharp increase in the derived count rate at the point of aggregate formation, the intersection method was thought to be less appropriate to determine the CAC compared to the second derivative method in the data sets gathered in this study. As shown in Figure 1, the intersection method failed to accurately pick out the point at which the light scattering of the solution first started to increase dramatically and therefore it was thought to be consistently overestimating the CAC concentration.

The fluorescence spectroscopy measurements were able to detect aggregation in the  $\mu\text{M}$  region (Table 1). When the second derivative method was applied, the CACs significantly decreased ( $p < 0.05$ ) from 16 to 10  $\mu\text{M}$  as pH increased from 4 to 8. When the CACs were calculated using the intersection method (Fig. 1), the CACs also significantly

decreased ( $p < 0.05$ ) from 11.06  $\mu\text{M}$  in pH 4 to 7.38  $\mu\text{M}$  in the pH 8 vehicle. Unlike the light scattering data, the fluorescence data analysis did not seem particularly sensitive to the method used to determine CAC and both were considered to be accurate methods to collect the data. The wavelength at which maximum fluorescence intensity occurred in the collected fluorescence spectra experienced a significant blue shift ( $p < 0.05$ ) from 373 nm in pH 4 to 361 nm in pH 8 (Table 1, refer to supporting information for fluorescence spectrum).

To probe the bonds formed between the aggregates in different tetracaine ionisation states, FTIR was employed. Based on the different CACs in different pH adjusted vehicles (Table 1), 100 mM of tetracaine was dispersed in pH 4 and 10 mM of tetracaine was dispersed in pH 8 to ensure that the FTIR measurements were analysing solutions with a high proportion of aggregates. The FTIR spectrum recorded for the tetracaine solutions showed significant visible shifts in the regions of interest (Fig. 2). The absorbance spectrum was normalised by the absorbance value at the  $\text{CH}_3$  region ( $2939\text{ cm}^{-1}$ ) to correct for the possibility of different laser intensities when performing the measurements. As the pH increased from 4 to 8, a reduction in intensity of carbonyl group peaks ( $1690$  and  $1606\text{ cm}^{-1}$ ) and **N-H bend** ( $1526\text{ cm}^{-1}$ ) was observed. An increase in intensity at the region associated with carboxylate groups were formed ( $1469\text{ cm}^{-1}$ ) was also observed.



## Tetracaine transport

Since each CAC referred to a change in the solution state equilibrium, it was suggested that multiple critical points in the spectroscopy data that characterised the aggregates was a consequence of a different arrangement of the molecules in the solution. In accordance with this interpretation at a tetracaine concentration of 16 and 50  $\mu\text{M}$ , at which two different forms of aggregates of tetracaine were thought to dominate in solution respectively at pH 4 (Table 1), were used as donor solutions for the transport studies to assess the effect of drug aggregation on membrane permeation.

At a solution pH of 4, the permeability coefficient through the porcine epidermis significantly decreased ( $p < 0.05$ ) from  $13.7 \pm 4.3$  to  $0.06 \pm 0.6 \times 10^{-3}$  cm/h when the tetracaine concentration increased from 10  $\mu\text{M}$  to 1.05 M (drug saturation). When the same test solutions were applied to the silicone membrane, a significant decrease ( $p < 0.05$ ) from  $0.7 \pm 0.2 \times 10^{-3}$  cm/h at 10  $\mu\text{M}$  to  $0.034 \pm 0.005 \times 10^{-3}$  cm/h at saturated tetracaine concentration was observed. Across the 10  $\mu\text{M}$  to 1000  $\mu\text{M}$  concentration range, where aggregates were thought to be present and change in properties (Table 1), the permeability coefficient through the silicone membrane remained unchanged ( $p > 0.05$ ) (Table 2, refer to supporting information for permeation profiles). The concentrations at which no change was observed in the silicone membrane were not tested in the porcine skin.

A different trend was observed in the permeation data when the pH was increased from pH 4 to pH 8 (Table 3, refer to supporting information for permeation profiles). The permeability coefficient through the porcine epidermis significantly increased ( $p < 0.05$ ) from  $29.9 \pm 9.9$  to  $75.1 \pm 41.7 \times 10^{-3}$  cm/h as the tetracaine concentration increased from 10  $\mu$ M to 6.29 mM (saturated concentration) (Fig. 3). In the silicone membrane, the permeability coefficient also significantly increased ( $p < 0.05$ ) from  $23.5 \pm 6.2$  to  $201.5 \pm 38.2 \times 10^{-3}$  cm/h. Unlike at pH 4, at pH 8 the increase in permeability coefficient seemed to occur gradually as the drug concentration was increased (i.e. at 40  $\mu$ M tetracaine donor solution the  $K_p$  was  $48.1 \pm 5.4 \times 10^{-3}$  cm/h).

## **Discussion**

### Tetracaine solution state interactions

Tetracaine, also known as amethocaine, is an amphiphilic molecule which presents a positive charge at physiological pH. The drug's chemical structure displays a hydrophilic region (amine portion) and a hydrophobic region (aromatic portion) and this predisposes the molecule to self-association in aqueous solution. At concentrations of more than 1 mM, previous literature suggests tetracaine forms an aggregate [31-33], but there appears to be a difference of opinion in the literature as to whether tetracaine forms organised micelles [34-36] or random molecular aggregates [31, 37].

There have been several studies that document tetracaine's critical aggregation constant

(CAC). For example, Kitagawa et al. proposed tetracaine hydrochloride had a CAC of 38 mM at 25 °C in an aqueous solution within the pH range of 4.5 to 5.7 [34] using an electrode method. A higher value of 128 mM was reported when surface tension, density and Kraft point measurements were used to determine the tetracaine CAC at pH 5.0 – 5.5 [35, 38, 39]. The inconsistency of these previously reported tetracaine CAC values may be due to technical issues in performing the experiments, but it is more likely the variance is a consequence of the different analytical equipment used to determine the CACs. It is notable that both the analytical techniques reported in these previous studies have a relatively high limit of detection, i.e. in the mM range [31, 34, 36, 40, 41]. If the tetracaine aggregation process is not uniform, i.e. it does not form a set of homogeneous micelles, it is possible that aggregation could start at much lower concentrations and the techniques previously employed to characterise tetracaine aggregation in previous work may have been only captures aggregation events at higher concentration. The results gathered from photon correlation spectroscopy in the current study, which also has relatively high limit of detection for molecular aggregates, supports the theory that the previously reported values for CAC were probably aggregation changes rather than the initial aggregation event because the CAC results at pH 4 (40 and 200 mM) were close to those reported previously in the literature [34, 35, 38, 39]. The CAC of tetracaine at pH 8 does not appear to have been investigated before and therefore, no comparisons with the literature values could be made. The fluorescence spectroscopy used in the current study probes a lower range of concentrations compared to photon correlation spectroscopy and thus, it provides useful additional information that supplements the literature in this field. In this study it showed a change in tetracaine conformation in solution at 16  $\mu$ M in pH 4

and 10  $\mu\text{M}$  in pH 8. The lower values recorded in the fluorescence measurements for the CAC compared to the photon correlation spectroscopy experiments supported the notion that the latter was not actually recording the first aggregation event, i.e. the CAC but rather changes in the confirmation of aggregates that were already present in solution. The fluorescence method detects tetracaine aggregation as a consequence of the shielding of the electrons in the aromatic ring, which generates signal quenching, when tetracaine molecules come together. The deviation from linearity in the concentration titration experiments signified a quenching process and this was interpreted, at the low concentration used in this study, as aggregation. At higher drug concentrations, signal quenching can occur simply as a consequence of an increase in drug molecules in solution. However, as an off-centre cell and very low concentrations of tetracaine was used to avoid these effects. The ability of the fluorescence measurements to detect conformation changes, which lead to aggregation, was supported by the spectral shift in wavelength observed when the pH of the solution in which the drug was dissolved changed.

Both photon correlation spectroscopy and fluorescence spectroscopy results showed that as the pH of the solution within which the tetracaine was dissolved increased, the critical points at which the aggregation events that the spectroscopy methods detected decreased. This phenomenon has been previously shown for other drug molecules. Attwood and Natarajan observed a higher critical micelle concentration at a low pH (0.5 – 5.5) in 5 different piperazine drugs (trifluoperazine, opipramol, thiopropazate, flupenthixol and clopenthixol) [42]. The structure of trifluoperazine is close to tetracaine. It has an

aromatic hydrocarbon and two nitrogen atoms which protonates at  $pK_a$  3.8 and 8.4. According to Attwood and Natarjan, the increase in CMC as pH decreases can be attributed to the increase in electrical charge of the molecule as the nitrogen atoms become protonated, which provides more pronounced amphiphilic properties and thus a greater propensity to form aggregates [42].

Both the fluorescence and FTIR studies seemed to suggest that tetracaine ionization influenced the type of aggregates that were formed by the drug. In pH 8, the tetracaine aggregates included a significant proportion of unionized tetracaine molecules. These unionised molecules seemed to generate a more hydrophobic environment when they were encouraged to form aggregates according given the blue fluorescence wavelength shift in the fluorescence spectra at pH 8, but not at pH 4 (Table 1). A similar trend has previously been observed by Mertz et al. [43], who showed a fluorescence blue shift when tetracaine aggregates were subjected to molecules that were known to form hydrogen bonds. The infrared spectra analysis of the data collected in the current work suggested that the drug aggregates formed in the pH 8 vehicle were formed by the generation of stronger intramolecular bonding because the carbonyl bands of tetracaine in pH 8 decreased more in intensity as a consequence of aggregation compared to pH 4. An investigation by Guerin et al. observed a similar decrease in carbonyl band intensity, but they were also able to a decrease in the drug's amine group peak intensity. This led to the hypothesis that tetracaine associated by stacking of the aromatic rings, involving mostly  $N-H \cdots N$  tertiary association with some  $N-H \cdots C=O$  ester and  $N-H \cdots N-H$  bonds [44]. The amine bond could not be detected in the current study but it was

assumed that a similar interaction occurred between the tetracaine molecules in this work.

Tetracaine is formulated at 0.15 M in commercially available topical products and hence, given the data reported in this study, it is likely that a significant proportion of the drug is presented to the human skin as aggregates when applied in the aqueous vehicles that are currently used to deliver this agent. It is therefore probable that the transport of a tetracaine product is significantly influenced by the aggregation state of the drug. Previous work has even suggested that drug aggregation may be the cause of the high lag time and low penetrating amount of tetracaine [16].

#### Tetracaine transmembrane permeation

The process of passive transmembrane penetration is commonly interpreted using Fick's second law of diffusion which makes the assumption that the system is homogeneous, i.e., there are no 'specific interactions' between the components of the system (drug, vehicle and membrane) [45-47]. According to Fick's second law of diffusion the permeability coefficient should be constant for a drug when changing the initial loading concentration of the permeating compound. Hence, any changes in permeability coefficient represent deviations from ideal scenario described by Fick's law, which can be a consequence of drug-membrane, drug-vehicle or drug-drug interactions.

The manner in which a molecule aggregates is a consequence of the free energy changes associated with the aggregated and non-aggregated forms of the drug. An equilibration

between non-aggregates and aggregates always exists in the solution state. Given its  $pK_a$ , in aqueous solutions at pH 4, aggregates are most likely to be formed of charged tetracaine molecules. This has been substantiated by previous zeta potential measurements, which has demonstrated that the aggregates are positively charged in an aqueous solution [16]. There are two main hypotheses that can be generated to explain the decrease in the permeability coefficient of the drug when charged tetracaine aggregates were formed. One possible hypothesis is that tetracaine transport was driven by only non-aggregated molecules. As the concentration of tetracaine in the solution increased, more aggregation occurred and hence there was less availability of free molecules. Thus, the permeability of tetracaine decreased. Another possible hypothesis is that tetracaine transport was driven by both aggregates and non-aggregates. Charged molecules often permeate through the skin via the shunt route and it is possible that the charged tetracaine aggregates followed this pathway [48]. Hence, when aggregation occurred perhaps more of the tetracaine molecules followed the shunt pathway and, as this has a limited capacity for molecule transport unlike the passive transport through the cell barrier it slowed the overall permeation rate. Of these two hypotheses, the former is more likely owing to the similar trends obtained from silicone membrane and porcine skin, which suggested (as silicone does not have any pores) that the shunt route was not a major route of transport that was modified by molecular aggregation in this study.

As there were a significant proportion of the tetracaine molecules that were uncharged when dissolved in an aqueous vehicle at pH 8, it was assumed that the aggregates formed at this pH were more hydrophobic than at pH 4. It may be possible that small uncharged

tetracaine aggregates could travel directly into the skin [49, 50]. The similar trend of increased permeation coefficient through the porcine membrane and silicone membrane suggests that aggregates do not travel through the shunt route and that a non-follicular route is favoured. There are two possible hypotheses to explain the increase in the permeability coefficient of tetracaine when aggregates were formed. The first hypothesis considers the monomers to be the only type of molecules which penetrates through the barrier. According to standard aggregation kinetics, to balance the dynamic equilibrium between the monomers and aggregates in the donor solution, when the monomers pass through the skin more aggregates dissociate into monomers to replenish the monomers that have entered the barrier. It may be the more hydrophobic aggregates have a greater propensity to supply the monomers quickly compared to the charged aggregates, which may have a low free energy in the polar solvent. While this hypothesis seems appealing, it fails on one critical aspect. The time to transport tetracaine across the *stratum corneum* is much slower than the time for aggregates to dissociate (around  $10^{-4}$  to 10 s) [51]. As such, the rate-determining step of tetracaine diffusion through the skin should be controlled by the rate of tetracaine transport through the *stratum corneum*, not the rate of aggregate dissolution. The second hypothesis is that tetracaine transport is driven by both aggregates and non-aggregates [21]. An increase in tetracaine concentration provides a supply of both monomers and aggregates. If both of these molecules pass through the skin directly via a non-follicular route, it would result in an increase in permeability of tetracaine. Further work is needed to confirm this hypothesis, but in order to do this, a method to detect how very small aggregates interact with the skin is needed.



## **Conclusions**

Tetracaine appeared to form aggregates in aqueous solutions in the  $\mu\text{M}$  range and this suggested that previous attempts to define the CAC in the mM concentration range may have been hindered by the limit of detection of the analytical equipment employed in the study. At different ionisation states, the type of aggregates formed differed. In a pH 4 vehicle, aggregates decreased tetracaine permeability coefficient but using pH 8, aggregates had the opposite effect. Thus, it seems plausible that the modification of drug aggregation could be an effective strategy to enhance tetracaine permeation through the skin. However, a detailed investigation of the effects of aggregation on drug transport at different concentrations should be performed. The importance of drug concentration was shown in this work through a comparison of the results obtained in the current study, at low tetracaine, concentrations, compared to those obtained at high tetracaine concentrations in previous studies [16]. It appeared that molecular aggregation had a more pronounced effect at lower concentrations and this should be considered when developing new topical formulations that employ molecules that have propensity to self-associate.

## **Acknowledgements**

We would like to thank Raquel Teixeira, Aateka Patel and Faiza Benaouda for teaching the use of fluorescence spectroscopy, FTIR and Franz cells.

## References

1. Zhang, J., et al., *The effect of solute-membrane interaction on solute permeation under supersaturated conditions*. International journal of pharmaceutics, 2012.
2. Benaouda, F., et al., *Discriminating the molecular identity and function of discreet supramolecular structures in topical pharmaceutical formulations*. Molecular Pharmaceutics, 2012.
3. Benaouda, F., et al., *Triggered In Situ Drug Supersaturation and Hydrophilic Matrix Self-Assembly*. Pharmaceutical Research, 2012: p. 1-9.
4. Attwood, D., *The mode of association of amphiphilic drugs in aqueous solution*. Advances in colloid and interface science, 1995. **55**: p. 271-303.
5. Schreier, S., S.V. Malheiros, and E. de Paula, *Surface active drugs: self-association and interaction with membranes and surfactants. Physicochemical and biological aspects*. Biochimica et Biophysica Acta (BBA)-Biomembranes, 2000. **1508**(1): p. 210-234.
6. Wyn-Jones, E. and J. Gormally, *Aggregation processes in solution*. Vol. 26. 1983: Elsevier Science Ltd.
7. Potts, R.O. and R.H. Guy, *Predicting skin permeability*. Pharmaceutical research, 1992. **9**(5): p. 663-669.
8. Bos, J.D. and M.M. Meinardi, *The 500 Dalton rule for the skin penetration of chemical compounds and drugs*. Experimental dermatology, 2000. **9**(3): p. 165-169.
9. Shore, P.A., B.B. Brodie, and C.A.M. Hogben, *The gastric secretion of drugs: a pH partition hypothesis*. Journal of Pharmacology and Experimental Therapeutics, 1957. **119**(3): p. 361-369.
10. Potts, R.O. and R.H. Guy, *A predictive algorithm for skin permeability: the effects of molecular size and hydrogen bond activity*. Pharmaceutical research, 1995. **12**(11): p. 1628-1633.
11. Alvarez-Roman, R., et al., *Skin penetration and distribution of polymeric nanoparticles*. J Control Release, 2004. **99**(1): p. 53-62.
12. Lademann, J., et al., *Nanoparticles - An efficient carrier for drug delivery into the hair follicles*. European Journal of Pharmaceutics and Biopharmaceutics, 2007. **66**: p. 159-164.
13. Wu, X., G.J. Price, and R.H. Guy, *Disposition of nanoparticles and an associated lipophilic permeant following topical application to the skin*. Mol Pharm, 2009. **6**(5): p. 1441-8.
14. Baroli, B., et al., *Penetration of metallic nanoparticles in human full-thickness skin*. Journal of Investigative Dermatology, 2007. **127**: p. 1701-1712.
15. Ryman-Rasmussen, J.P., J.E. Riviere, and N.A. Monteiro-Riviere, *Penetration of intact skin by quantum dots with diverse physicochemical properties*. Toxicological Sciences, 2006. **91**: p. 159-165.
16. Inacio, R., et al., *Investigating how the attribute of self-associated drug complexes influence the passive transport of molecules through biological membranes*. European Journal of Pharmaceutics and Biopharmaceutics, In-press.

17. Charman, W.N., et al., *Self-association of nicotinamide in aqueous-solution - mass-transport, freezing-point depression, and partition-coefficient studies*. Pharmaceutical Research, 1991. **8**(9): p. 1144-1150.
18. Mikkelsen, T.J., et al., *Effect of self-association of phenol on its transport across polyethylene film*. Journal of Pharmaceutical Sciences, 1980. **69**(2): p. 133-137.
19. James-Smith, M., et al., *Effect of Surfactant Mixtures on Skin Structure and Barrier Properties*. Annals of Biomedical Engineering, 2011. **39**(4): p. 1215-1223.
20. Higuchi, T., *Physical chemical analysis of percutaneous absorption process from creams and ointments*. J. Soc. Cosmet. Chem, 1960. **11**: p. 85-97.
21. Moore, P.N., S. Puvvada, and D. Blankschtein, *Challenging the surfactant monomer skin penetration model: Penetration of sodium dodecyl sulfate micelles into the epidermis*. Journal of Cosmetic Science, 2003. **54**(1): p. 29-46.
22. Moore, P.N., et al., *Penetration of mixed micelles into the epidermis: Effect of mixing sodium dodecyl sulfate with dodecyl hexa(ethylene oxide)*. Journal of Cosmetic Science, 2003. **54**(2): p. 143-159.
23. Committee, J.F., *British National Formulary*. 2012, BMJ Group and Pharmaceutical Press: London.
24. Lakowicz, J.R., *Principles of fluorescence spectroscopy*. 2009: Springer.
25. Albani, J.R., *Principles and applications of fluorescence spectroscopy*. 2008: Wiley-Blackwell.
26. Khan, A.M. and S.S. Shah, *Determination of critical micelle concentration (Cmc) of sodium dodecyl sulfate (SDS) and the effect of low concentration of pyrene on its Cmc using ORIGIN software*. Journal of the Chemical Society of Pakistan, 2008. **30**(2): p. 186-191.
27. Mukerjee, P.a.M., Karol J, *Critical Micelle Concentrations of Aqueous Surfactant Systems: By Pasupati Mukerjee and Karol J. Mysels*. 1971: National Bureau of Standards.
28. Kligman, A.M. and E. Christophel, *Preparation of isolated sheets of human stratum corneum*. Archives of Dermatology, 1963. **88**: p. 702-&.
29. Harrison, S.M., B.W. Barry, and P.H. Dugard, *Effects of freezing on human-skin permeability*. Journal of Pharmacy and Pharmacology, 1984. **36**: p. 261-262.
30. Williams, A., *Transdermal and topical drug delivery: From theory to clinical practice*. 2003: Pharmaceutical Press London.
31. Farhadieh, B., N.A. Hall, and E. Hammarlund, *Aggregation of certain medicinal amines in aqueous solutions of their salts*. Journal of Pharmaceutical Sciences, 1967. **56**(1): p. 18-23.
32. Florence, A.T. and D. Attwood, *Physicochemical principles of pharmacy*. 2011: Pharmaceutical Pr.
33. Johnson, E. and D. Ludlum, *Aggregation of local anesthetics in solution*. Biochemical pharmacology, 1969. **18**(10): p. 2675.
34. Kitagawa, N., M. Oda, and T. Totoki, *Possible mechanism of irreversible nerve injury caused by local anesthetics: detergent properties of local anesthetics and membrane disruption*. Anesthesiology, 2004. **100**(4): p. 962-967.

35. Matsuki, H., et al., *Differential scanning calorimetric study on the Krafft phenomenon of local anesthetics*. Journal of colloid and interface science, 1996. **181**(2): p. 362-369.
36. Shaikh, V.R., et al., *Volumetric studies of aqueous solutions of local anaesthetic drug compounds [hydrochlorides of procaine (PC HCl), lidocaine (LC HCl) and tetracaine (TC HCl)] at 298.15 K*. Journal of Molecular Liquids, 2011. **164**(3): p. 239-242.
37. Attwood, D. and P. Fletcher, *Self-association of local anaesthetic drugs in aqueous solution*. Journal of pharmacy and pharmacology, 1986. **38**(7): p. 494-498.
38. Matsuki, H., et al., *Surface adsorption and volume behavior of local anesthetics*. Langmuir, 1994. **10**(6): p. 1882-1887.
39. Miller, K., et al., *Importance of molecular aggregation in the development of a topical local anesthetic*. Langmuir, 1993. **9**(1): p. 105-109.
40. Umemura, J. and H.H. Mantsch, *The Molecular Association of Tetracaine with Ethylpalmitate: An Infrared Spectroscopic Study*. Bulletin of the Institute for Chemical Research, Kyoto University, 1981. **58**(5-6): p. 548-554.
41. Guerin, M., J.-M. Dumas, and C. Sandorfy, *Vibrational spectroscopic studies of molecular associations by local anesthetics*. Canadian Journal of Chemistry, 1980. **58**(19): p. 2080-2088.
42. Attwood, D. and R. Natarajan, *Effect of pH on the micellar properties of amphiphilic drugs in aqueous-solution*. Journal of Pharmacy and Pharmacology, 1981. **33**(3): p. 136-140.
43. Mertz, C., et al., *Photophysical studies of local anesthetics, tetracaine and procaine: drug aggregations*. Photochemistry and photobiology, 1990. **51**(4): p. 427-437.
44. Guérin, M., J.-M. Dumas, and C. Sandorfy, *Vibrational spectroscopic studies of molecular associations by local anesthetics*. Canadian Journal of Chemistry, 1980. **58**(19): p. 2080-2088.
45. Mitragotri, S., et al., *Mathematical models of skin permeability: an overview*. International journal of pharmaceutics, 2011. **418**(1): p. 115-129.
46. Godin, B. and E. Touitou, *Transdermal skin delivery: Predictions for humans from in vivo, ex vivo and animal models*. Advanced Drug Delivery Reviews, 2007. **59**(11): p. 1152-1161.
47. Kalia, Y.N. and R.H. Guy, *Modeling transdermal drug release*. Advanced Drug Delivery Reviews, 2001. **48**(2-3): p. 159-172.
48. Edwards, D.A. and R. Langer, *A linear-theory of transdermal transport phenomena*. Journal of Pharmaceutical Sciences, 1994. **83**(9): p. 1315-1334.
49. Abraham, M.H., H.S. Chadha, and R.C. Mitchell, *The factors that influence skin penetration of solutes*. Journal of Pharmacy and Pharmacology, 1995. **47**(1): p. 8-16.
50. Pugh, W.J., M.S. Roberts, and J. Hadgraft, *Epidermal permeability - Penetrant structure relationships .3. The effect of hydrogen bonding interactions and molecular size on diffusion across the stratum corneum*. International Journal of Pharmaceutics, 1996. **138**(2): p. 149-165.

51. Patist, A., et al., *Importance of micellar relaxation time on detergent properties*. *Journal of Surfactants and Detergents*, 1999. **2**(3): p. 317-324.

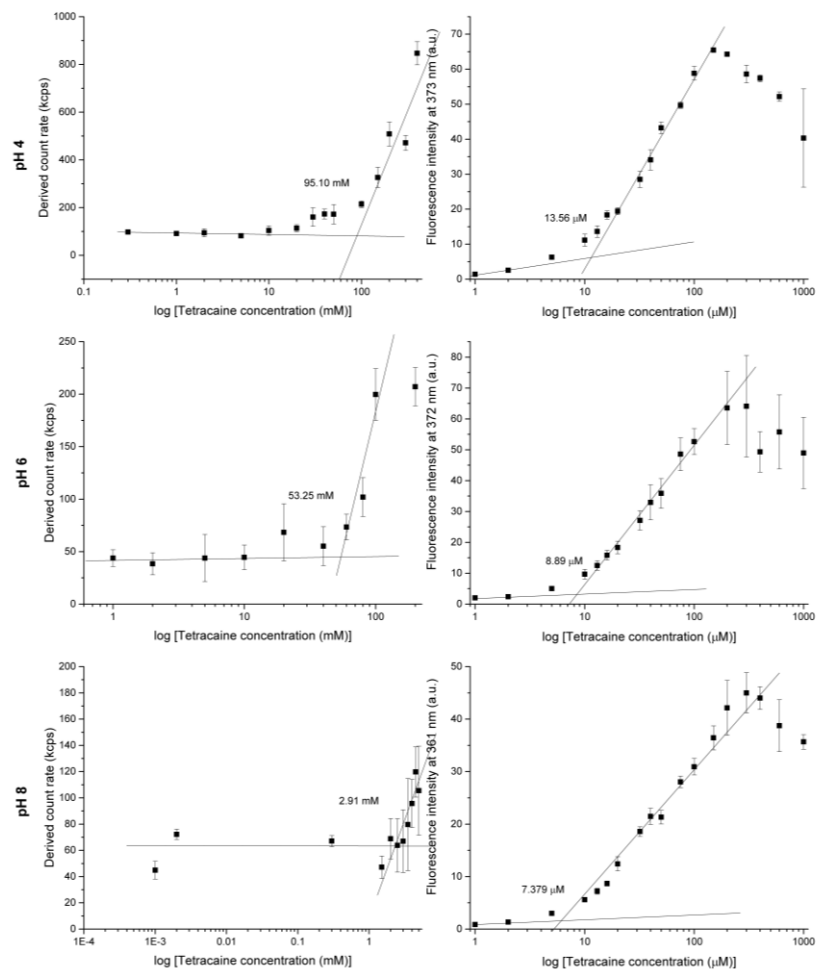


**Fig. 1.** Graphs depicting critical aggregation constants (CACs) using photon correlation spectroscopy (left) and fluorescence spectroscopy (right) in pH 4, 6 and 8.

pH	Critical aggregation constants (CACs) using photon correlation spectroscopy (mM)		Critical aggregation constants (CACs) using fluorescence spectroscopy ( $\mu\text{M}$ )		$\lambda_{\text{max}}$ (nm)
	Second derivative test	Intersection of 2 linear slopes	Second derivative test	Intersection of 2 linear slopes	
4	40, 200	95.10	16, 50, 600	11.06	373
6	20, 100	53.25	16, 40	8.89	372
8	0.3, 2	2.91	10, 32, 100, 200	7.38	361

**Table 1.** Characteristics of tetracaine aggregation in different pHs using fluorescence spectroscopy and photon correlation spectroscopy, where  $\lambda_{\text{max}}$  represents the wavelength at which maximum fluorescence intensity occurs.

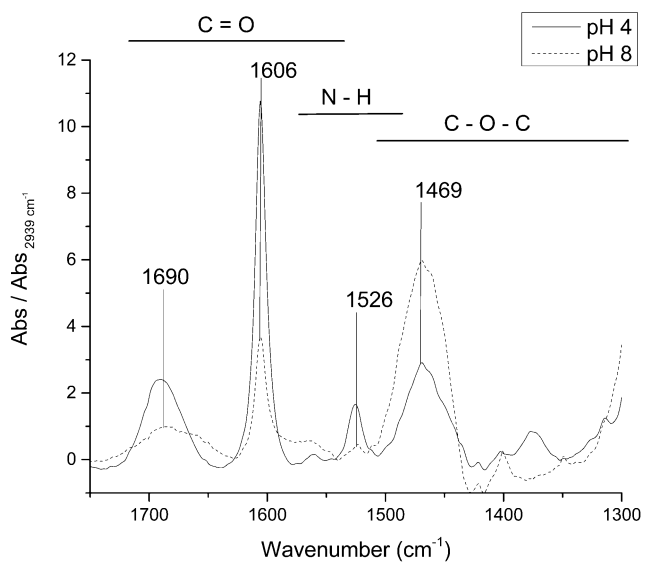


**Fig. 2.** FTIR data of tetracaine in pH 4 and 8.



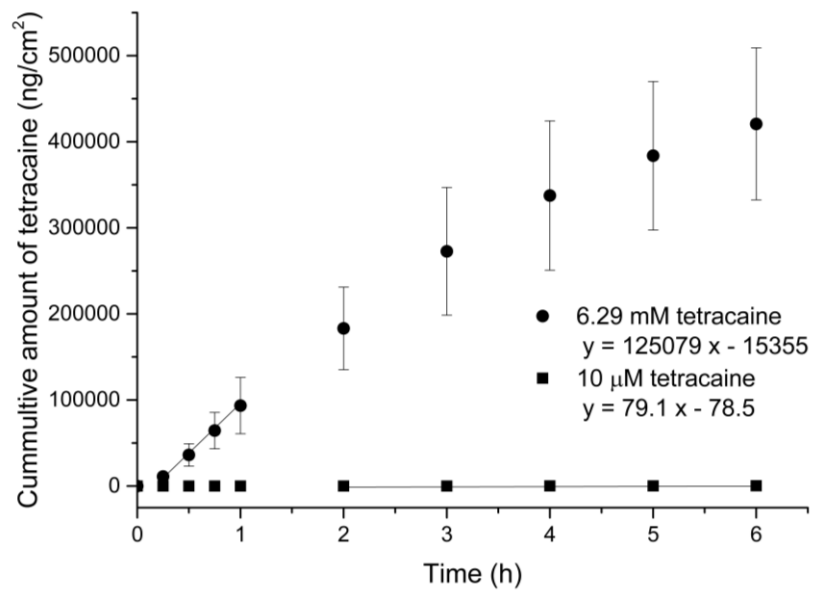


**Fig. 3.** Permeation profile of various concentrations of tetracaine through porcine epidermis at pH 8. Each point represents mean  $\pm$ standard deviation (n=5).

Concentration ( $\mu\text{M}$ )	Porcine epidermis		0.12 mm silicone membrane	
	Flux ( $\text{ng}/\text{cm}^2/\text{h}$ )	$K_p$ ( $10^{-3} \text{ cm}/\text{h}$ )	Flux ( $\text{ng}/\text{cm}^2/\text{h}$ )	$K_p$ ( $10^{-3} \text{ cm}/\text{h}$ )
10	$36.2 \pm 11.3$	$13.7 \pm 4.3$	$2.0 \pm 0.6$	$0.7 \pm 0.2$
20	-	-	$3.4 \pm 0.7$	$0.7 \pm 0.1$
40	-	-	$9.4 \pm 0.7$	$0.8 \pm 0.1$
100	-	-	$13.6 \pm 3.3$	$0.5 \pm 0.1$
1000	-	-	$177.9 \pm 44.6$	$0.7 \pm 0.2$
$1.05 \times 10^6$	$(1.6 \pm 0.6) \times 10^4$	$0.06 \pm 0.02$	$(9.4 \pm 1.4) \times 10^3$	$0.034 \pm 0.005^*$

**Table 2.** Steady state flux and permeability coefficients,  $K_p$ , of different concentrations of tetracaine in pH 4 across porcine epidermis and silicone membrane. Data represent mean  $\pm$  standard deviation of 3 independent tetracaine samples. \* Significant differences were observed based on Games Howell test.

Concentration ( $\mu\text{M}$ )	Porcine epidermis		0.25 mm silicone membrane	
	Flux ( $\text{ng}/\text{cm}^2/\text{h}$ )	$K_p$ ( $10^{-3} \text{ cm}/\text{h}$ )	Flux ( $\text{ng}/\text{cm}^2/\text{h}$ )	$K_p$ ( $10^{-3} \text{ cm}/\text{h}$ )
10	$79.1 \pm 26.1$	$29.9 \pm 9.9$	$62.2 \pm 16.5$	$23.5 \pm 6.2$
40	-	-	$508.5 \pm 56.9$	$48.1 \pm 5.4$
$6.29 \times 10^3$	$(1.2 \pm 0.7) \times 10^5$	$75.1 \pm 41.7$	$(3.4 \pm 0.6) \times 10^5$	$201.5 \pm 38.2$

**Table 3.** Steady state flux and permeability constants,  $K_p$ , of different concentrations of tetracaine in pH 8 across porcine epidermis and silicone membrane. Data represent mean  $\pm$  standard deviation of 3 independent tetracaine samples. \* Significant differences were observed based on Games Howell test.